Scheme I

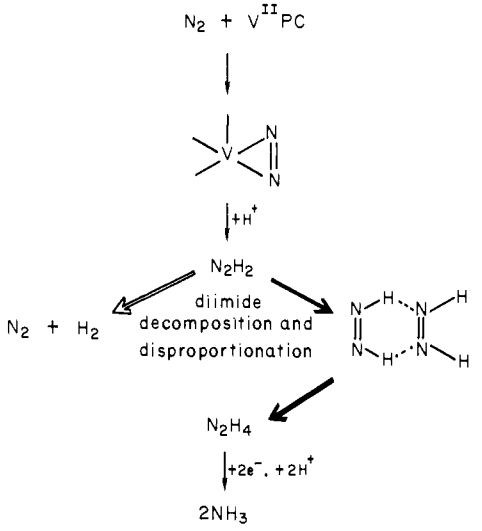

is the product of hydrolysis of an intermediate complex. They also argued that N_2H_4 is formed outside the main path of N_2 reduction to NH_3. Assuming that N_2 is reduced directly to NH_3, they concluded that only 1% of the N_2 is reduced via N_2H_4.[10]

The experiment from ref 10 is reproduced in Figure 9. *It is actually a diimide-trapping experiment*, and the observed results can be taken as a proof for the diimide mechanism of N_2 reduction proposed by us. It must first be mentioned that N_2H_4 is reduced ca. 100 times more rapidly than N_2 (see Table III) and that N_2H_4 therefore cannot accumulate in *reacting* solutions under any conditions.

However, if the reactions are stopped with acid, the N_2H_2 present in the solution at this moment can still disproportionate into N_2H_4 and N_2. Accordingly, the amounts of N_2H_4 detected at various time points are a measure of the stationary N_2H_2 concentration. The shape of the N_2H_4 disappearance function in Figure 9 indicates that N_2H_4 is the product of a second-order reaction. This result is typical for the kinetic behavior of N_2H_2 under conditions where its disproportionation into N_2H_4 and N_2 is the main reaction.[1,30]

We thus conclude that the "diimide mechanism" of N_2 reduction as proposed[1,2,24] from studies in the $V(OH)_2/Mg(OH)_2$– and molybdothiol systems (Scheme I) also applies to the reduction of N_2 by $V^{II}PC$.

Acknowledgment. This work was supported by Grants CHE76-10890 and CHE79-50003 from the National Science Foundation. We thank Craig Martin, Keith Pence, and Robert Deere for skillful experimental assistance.

(30) Willis, C.; Back, R. A. *Can. J. Chem.* **1973**, *51*, 3605.

Ferric Ion Sequestering Agents. 6.[1] The Spectrophotometric and Potentiometric Evaluation of Sulfonated Tricatecholate Ligands

Wesley R. Harris, Kenneth N. Raymond,* and Frederick L. Weitl

Contribution from the Department of Chemistry, University of California, Berkeley, California 94720. *Received June 30, 1980*

Abstract: Ferric ion complexation equilibria have been evaluated for the sulfonated tricatecholate ligands 1,3,5-tris[((2,3-dihydroxy-5-sulfobenzoyl)amino)methyl]benzene (MECAMS), 1,5,10-tris(2,3-dihydroxy-5-sulfobenzoyl)-1,5,10-triazadecane (3,4-LICAMS), 1,5,9-tris(2,3-dihydroxy-5-sulfobenzoyl)-1,5,9-cyclotriazatridecane (3,3,4-CYCAMS), and 1,3,5-tris[(2,3-dihydroxy-5-sulfobenzoyl)carbamido]benzene (TRIMCAMS). Protonation and formation constants have been determined by potentiometric and spectrophotometric techniques. The formation constants show that these ligands form exceptionally stable complexes with ferric ion (log $K_{ML} \approx 40$). The protonation studies have established that the complexes of MECAMS, 3,4-LICAMS, and 3,3,4-CYCAMS undergo a series of 1:1 protonation reactions which result in a shift in the mode of bonding from one in which the iron(III) is coordinated through the two phenolic oxygens of the dihydroxybenzoyl group (catecholate mode) to one in which the meta phenolic group is protonated and the iron(III) is bound through the ortho phenolic and amide carbonyl oxygens (salicylate mode). The results are discussed in relation to the chelation therapy of iron overload, as occurs in the treatment of Cooley's anemia.

The average adult contains 4–5 g of elemental iron, of which about 65% is present in the oxygen-transport protein hemoglobin and another 30% is stored in the iron-storage proteins ferritin or hemosiderin.[2] The transport of iron and the maintenance of free ferric ion concentrations at a low equilibrium value are accomplished by the iron-transport protein transferrin. However, despite the human body's ability to manage relatively high levels of iron, excessive amounts of this element are in fact quite toxic. Indeed, with the advent of iron-enriched vitamin supplements, acute iron overload has become one of the most common types of poisoning among young children.[3] Acute poisoning of adults is less common, but chronic iron overload is frequently encountered as a side effect of the regular transfusions of whole blood required by individuals suffering from β-thalassemia, a genetic disease characterized by the deficient production of the β chains of hemoglobin.[4] Such transfusions are necessary to maintain adequate hemoglobin levels—but since the body has no effective mechanism for excreting

(1) Part 5 in this series: Weitl, F. L.; Raymond, K. N.; Durbin, P. W. *J. Med. Chem.* **1981**, *24*, 203–206.
(2) Beck, W. S. "Hematology"; Massachusetts Institute of Technology, 1974; p 28.
(3) Robothan, J. L.; Troxler, R. F.; Lietman, P. S. *Lancet* **1974**, *2*, 664–665.
(4) Reference 2, p 211.

0002-7863/81/1503-2667$01.25/0

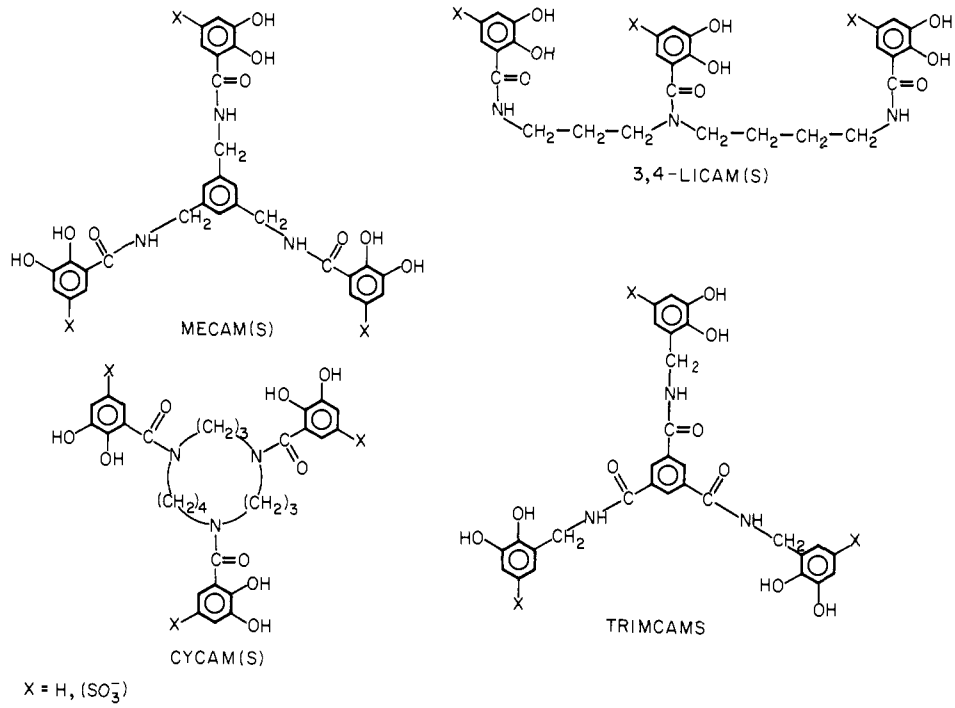

Figure 1. Structural formulas of catechoyl amide (CAM) ligands. The "S" is added to the basic form of the acronym when X = SO_3^-.

serum iron, the iron contained in the fresh blood (~250 mg/pint) is released upon hemolysis and eventually accumulates to lethal levels, primarily affecting the liver and heart.[5]

The excretion of metal ions can be enhanced by the administration of a suitable sequestering agent. The current drug of choice for iron removal is desferrioxamine B,[6] a linear trihydroxamic acid siderophore produced by several species of *Streptomyces* and *Norcardia*.[7] However, it is only capable of reducing iron levels to about 10 times normal values.[6] It must also be administered by injection and such injections are quite painful. Thus there is a genuine need for a more effective sequestering agent for clinical iron removal.

Enteric bacteria produce a second type of siderophore called enterobactin,[8,9] a cyclic triester of (2,3-dihydroxybenzoyl)-*l*-serine. We have previously shown that enterobactin forms exceptionally stable ferric complexes (log $K_{ML} \approx 52$)[10] and is capable of removing iron directly from transferrin much more effectively than does desferrioxamine B.[11] However, the ester linkages of enterobactin are slowly hydrolyzed at physiological conditions,[12] and the resulting (dihydroxybenzoyl)serine is a much less effective sequestering agent. If for no other reason, this makes enterobactin itself poorly suited for clinical use.

We have previously reported the synthesis and thermodynamic evaluation of two enterobactin analogues, 1,3,5-tris[((2,3-dihydroxybenzoyl)amino)methyl]benzene (MECAM) and 1,5,9-tris(2,3-dihydroxybenzoyl)-1,5,9-cyclotriazatridecane (3,3,4-CYCAM).[13] Like enterobactin, these ligands bind iron through the six phenolic oxygens of three 2,3-dihydroxybenzoyl groups and have a high affinity for ferric ion. Unlike enterobactin, they are hydrolytically stable, making them viable candidates for chelation therapy.

This paper reports the evaluation of four new sulfonated tricatecholate compounds: 1,3,5-tris[((2,3-dihydroxy-5-sulfobenzoyl)amino)methyl]benzene (MECAMS), 1,5,10-tris(2,3-dihydroxy-5-sulfobenzoyl)-1,5,10-triazadecane (3,4-LICAMS), 1,5,9-tris(2,3-dihydroxy-5-sulfobenzoyl)-1,5,9-cyclotriazatridecane (3,3,4-CYCAMS), and 1,3,5-tris[(2,3-dihydroxy-5-sulfobenzoyl)carbamido]benzene (TRIMCAMS). Structural formulas for these ligands are shown in Figure 1.

The sulfonation of these catecholate ligands is designed to serve a number of purposes. Most important, it substantially decreases the ligand protonation constants. Catechols are such weak acids that, even at neutral pH, competition from hydrogen ion is a significant factor which decreases the ability of the ligand to sequester iron. Thus by lowering the ligand protonation constants, one may increase the effectiveness of the ligand at physiological pH. Sulfonation also substantially increases the otherwise low water solubility of these types of ligands (enterobactin has a solubility of only 0.1 mM at pH 7).[14] In addition, the electron-withdrawing effect of the sulfonate group stabilizes the catecholate group against air oxidation. A preliminary report on the synthesis and evaluation of these ligands has already appeared.[15]

Experimental Section

Materials. Samples of each ligand were prepared according to the procedures described earlier.[15] Molecular weights were determined by potentiometric titration with KOH. Stock solutions of KOH and $Fe(NO_3)_3$ were prepared and standardized as previously described.[13]

Potentiometric and Spectrophotometric Measurements. The procedures and apparatus used for potentiometric measurements have been described previously in detail.[13] Briefly, measurements were made at 25 ± 0.05 °C and 0.10 M (KNO_3) ionic strength. The pH meter was standardized by titrations of HNO_3 and acetic acid to read $-\log [H^+]$ (where $[H^+]$ is the hydrogen ion *concentration*, not activity).

Competition Equilibria. Competition equilibria between ferric ion, EDTA, and the catecholate ligand were evaluated spectrophotometrically by measuring the absorbance of the ferric catecholate species. The pH

(5) Reference 2, p 211.
(6) Anderson, W. F.; Hiller, M. C., Eds. "Development of Iron Chelators for Clinical Use"; Department of Health, Education, and Welfare, 1975; Publication No. (NIH) 77-994.
(7) Neilands, J. B. *Struct. Bonding (Berlin)* **1966**, *1*, 59–108.
(8) O'Brien, I. G.; Gibson, F. *Biochim. Biophys. Acta* **1970**, *215*, 393–402.
(9) Pollack, J. R.; Neilands, J. B. *Biochem. Biophys. Res. Commun.* **1970**, *38*, 989–992.
(10) Harris, W. R.; Carrano, C. J.; Cooper, S. R.; Sofen, S. R.; Avdeef, A.; McArdle, J. V.; Raymond, K. N. *J. Am. Chem. Soc.* **1979**, *101*, 6097–6104.
(11) Carrano, C. J.; Raymond, K. N. *J. Am. Chem. Soc.* **1979**, *101*, 5401–5404.
(12) O'Brien, I. G.; Cox, G. B.; Gibson, F. *Biochim. Biophys. Acta* **1970**, *201*, 453.
(13) Harris, W. R.; Raymond, K. N. *J. Am. Chem. Soc.* **1979**, *101*, 6534–6541.
(14) O'Brien, I. G.; Gibson, F. *Biochim. Biophys. Acta* **1970**, *215*, 393–402.
(15) Weitl, F. L.; Harris, W. R.; Raymond, K. N. *J. Med. Chem.* **1979**, *22*, 1281–1283.

Table I. Protonation Constants of Sulfonated Catecholate Ligands

ligand	log K_4^H	log K_5^H	log K_6^H	av K_{4-6}^H
MECAMS	7.26	6.44	5.88	6.5
3,4-LICAMS	8.28	7.07	6.11	7.2
3,3,4-CYCAMS	8.56	7.80	7.01	7.8
TRIMCAMS	8.72	8.16	7.53	8.1
DMBS				7.26[a]

[a] $K_2^H = [H_2L]/([H][HL])$.

for each competition must be chosen so that the iron is evenly distributed between the catecholate ligand and the EDTA. Typically, competition experiments were run at pH 5–6.5. Protonation equilibria involving the free ligands and the ferric complexes are included in the calculations by using the protonation constants determined here or literature values for EDTA.

To ensure that true equilibrium was reached, duplicate reactions were run; in one case, the catecholate ligand was added to a solution of ferric EDTA, while in the second experiment EDTA was added to the ferric catecholate complex. Spectra were recorded 24–36 h after the solutions were mixed. During this time, the flasks were suspended in a 25 °C water bath. The satisfactory agreement in calculated log β values from the duplicate runs was taken as sufficient proof that the solutions had reached equilibrium.

Nonlinear Least Squares. The computer refinement of the potentiometric data was based on the minimization of the sum of the squares of the differences between observed and calculated pH values for each point in the titration which is sensitive to changes in any of the log β's. Between 15 and 30 data points were used for each log β which was varied.

Given an initial set of guesses for the log β's, values for pH, pL, and pM were calculated for each data point by varying these parameters to minimize the differences between calculated and analytical concentrations of total hydrogen, total ligand, and total metal. The residual for each data point is $R^2 = W^2(pH_{calcd} - pH_{obsd})^2$. At the end of each cycle, the set of log β values is changed to minimize the sum of the residuals using analytical derivatives for $\partial \log \beta_i/\partial pH$, with $\log \beta_{new} = \log \beta_{old} + (\partial \log \beta_i/\partial pH)\Delta pH$.

The weighting factor was based on the estimated uncertainty in the pH reading at each point in the titration curve. This uncertainty has two components, the precision of the pH meter itself and the precision of titrant delivery. Thus the weight was calculated as

$$\frac{1}{W_i} = \sigma_{meter}^2 + \left(\frac{\partial pH}{\partial V_T}\right)_i^2 \sigma_{V_T}^2$$

where $\sigma_{meter} = 0.003$ pH unit, $\sigma_{V_T} = 0.002$ mL, and $\partial pH/\partial V_T$ is the slope of the titration curve at each point in the titration. This system emphasizes the more accurate data from buffer regions and minimizes the relatively inaccurate pH readings from the steep inflections.

Results

Ligand Protonation Constants. Catechol is a very weak diprotic acid, with widely separated successive protonation constants for the two phenolic oxygens. The initial protonation of the catecholate dianion has an equilibrium constant[16] of $\log K_1^H = 13$ for reaction 1.

$$H^+ + cat^{2-} \rightleftharpoons Hcat^- \quad (1)$$

The second protonation constant is much lower, with $\log K_2^H = 9.2$ for eq 2. Because of this large difference in the intrinsic

$$H^+ + Hcat^- \rightleftharpoons H_2cat \quad (2)$$

acidity of catecholate oxygens, the six dissociable protons of the tricatecholate ligands clearly divide into two groups of three. The first group have an average protonation constant of around 10^7. These are listed in Table I, where K_n^H is defined in eq 3.

$$K_n^H = [H_nL]/([H_{n-1}L][H]) \quad (3)$$

These values represent the second (more acidic) protonation of the phenolic oxygens on each of the three catecholate groups.

(16) Martell, A. E.; Smith, R. M. "Critical Stability Constants"; Plenum Press: New York, 1977.

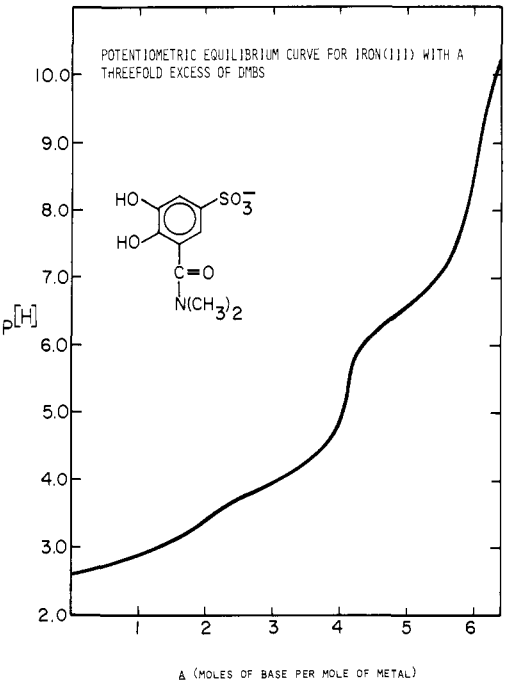

Figure 2. Potentiometric equilibrium curve for a 1:3 solution of ferric ion and 2,3-dihydroxy-5-sulfo-*N*,*N*-dimethylbenzamide (DMBS): $[Fe^{3+}]_{total} = 1.3 \times 10^{-3}$ M; $\mu = 0.10$ M (KNO_3); $T = 25$ °C.

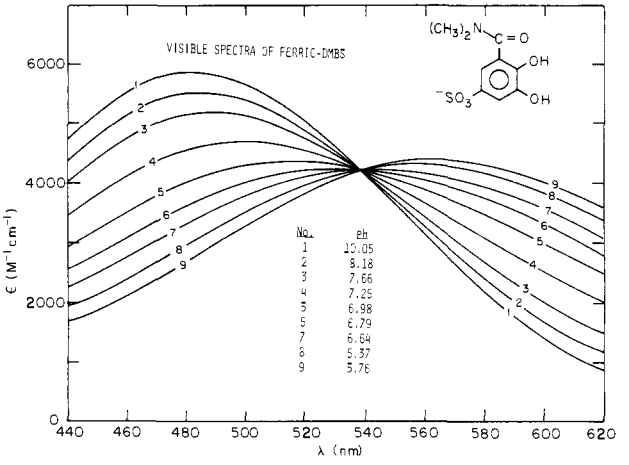

Figure 3. Visible spectra of a 1:3 solution of ferric ion and 2,3-dihydroxy-5-sulfo-*N*,*N*-dimethylbenzamide, recorded as a function of pH: $[Fe^{3+}]_{total} = 2 \times 10^{-4}$ M; $\mu = 0.10$ M (KNO_3); $T = 25$ °C.

The average values bracket $\log K_2^H$ of the bidentate analogue, 5-sulfo-2,3-dihydroxy-*N*,*N*-dimethylbenzamide (DMBS). The TRIMCAMS constants are higher due to the absence of an α-carbonyl functionality on the catechol rings, which lowers the first protonation constant by about 1 log unit.

The remaining three dissociable protons of the tricatecholate ligands are much less acidic, and the titration curves indicate no appreciable dissociation below pH 11. Therefore, no attempt was made to determine $\log K_n^H$ for $n = 1$–3.

Ferric DMBS. The potentiometric equilibrium curve of a 1:3 solution of ferric ion and DMBS is shown in Figure 2. Breaks at a values of 2, 4, and 6 indicate the formation of mono, bis, and tris ferric complexes of this H_2L ligand (a = moles of base added per mole of metal). The break at $a = 2$ is quite gentle, due to considerable overlap between the formation of the mono and bis complexes. However, the buffer region from $a = 4$ to $a = 6$ is well resolved, indicating that the reaction of the $(DMBS)_2Fe^{III}$ complex with a third DMBS ligand is well separated from the other complexation equilibria.

The visible spectra of the ferric DMBS system between pH 6 and pH 9 (a = 4–6) form a sharp isosbestic point at 537 nm

Table II. Proton-Dependent Stability Constants of Ferric DMBS Complexes

	potentiometric	spectrophotometric
$\log K_1$	7.23 (1)	
$\log K_2$	1.81 (4)	1.87 (8)
$\log K_3$	−3.21 (10)	−3.13 (14)

(Figure 3), indicating that there is a single complexation equilibrium present over this pH range. Above pH 9, λ_{max} is constant at 480 nm, which is characteristic of tris(catecholato)iron(III) complexes.[10,14,17] At pH 5.5 corresponding to $a = 4$, the λ_{max} has shifted to 563 nm, which is characteristic of bis(catecholato)iron(III) species.[17,18] Thus the spectra confirm that the two-equivalent buffer region between $a = 4$ and $a = 6$ in the titration curve reflects the addition of a third DMBS ligand to the $(DMBS)_2Fe^{III}$ complex.

The visible spectra at pH values just below $a = 4$ form a new isosbestic point at 678 nm, which presumably results from the equilibrium between FeDMBS and $Fe(DMBS)_2$ complexes. This isosbestic point disappears below pH 3.5 due to the complete dissociation of a small fraction of the 1:1 complex into free iron and ligand.

Because it is very difficult to obtain an accurate value for the higher ligand protonation constant of DMBS, we have chosen to describe the complexation equilibria by a series of proton-dependent equilibrium constants (eq 4–6).

$$Fe^{3+} + HDMBS^{2-} \rightleftharpoons FeDMBS + H^+ \quad (4)$$

$$K_1 = \frac{[FeDMBS][H]}{[Fe][HDMBS]}$$

$$FeDMBS + HDMBS^{2-} \rightleftharpoons Fe(DMBS)_2^{3-} + H^+ \quad (5)$$

$$K_2 = \frac{[Fe(DMBS)_2][H]}{[FeDMBS][HDMBS]}$$

$$Fe(DMBS)_2^{3-} + HDMBS^{2-} \rightleftharpoons Fe(DMBS)_3^{6-} + H^+ \quad (6)$$

$$K_3 = \frac{[Fe(DMBS)_3][H]}{[Fe(DMBS)_2][HDMBS]}$$

Although this convention is somewhat nonstandard, it avoids introducing considerable error due to inaccurate values of $\log K_1^H$ of the ligand. These proton-dependent constants are valid under any conditions where the concentration of fully deprotonated $DMBS^{3-}$ is negligible, i.e., below pH ≈ 10.5.

Values of K_1, K_2, and K_3 have been calculated by nonlinear least-squares refinement of the potentiometric data in which these three constants were the only parameters. The results are listed in Table II. In addition, K_2 and K_3 are readily obtained from the visible spectra, using data from those pH regions in which the presence of an isosbestic point indicates nonoverlapping complexation equilibria. Spectrophotometric values of $\log K_2$ and $\log K_3$ are also listed in Table II and are in excellent agreement with the potentiometric results.

Chelate Protonation Constants. All the tricatecholate ligands included in this study, 3,3,4-CYCAMS, 3,4-LICAMS, MECAMS, and TRIMCAMS, bind iron with such tenacity that there is essentially no free (unchelated) ferric ion present in these systems at pH values greater than 2. As a result, overall formation constants are not readily obtained from potentiometric data. Instead, these have been determined spectrophotometrically by a competition method described below.

Although there is no metal–ligand dissociation over the pH range accessible to potentiometric analysis, the titration curves in Figure 4 clearly show well-resolved buffer regions at intermediate pHs. Rather than representing ligand dissociation, these buffer regions reflect the stepwise protonation of the metal chelates. Because the chelate remains intact over the pH range of interest, the chelate protonation constants, defined as eq 7, can

$$K_{MH_nL} = [MH_nL]/([MH_{n-1}L][H]) \quad (7)$$

be determined in the same way that one would determine ligand protonation constants. The results for the various systems are described below.

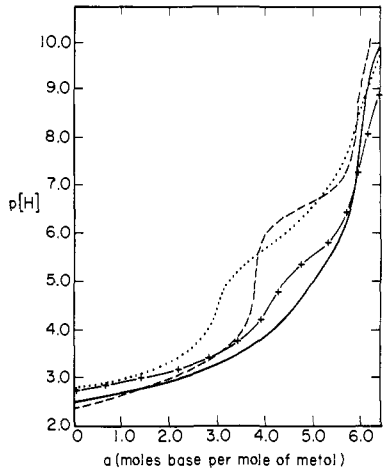

Figure 4. Potentiometric equilibrium curves for 1:1 solutions of ferric ion with MECAMS (—), 3,4-LICAMS (−+−), 3,3,4-CYCAMS (···), and TRIMCAMS (---): $[Fe^{3+}]_{total} \approx 1.3 \times 10^{-3}$ M; $\mu = 0.10$ M (KNO_3); T = 25 °C.

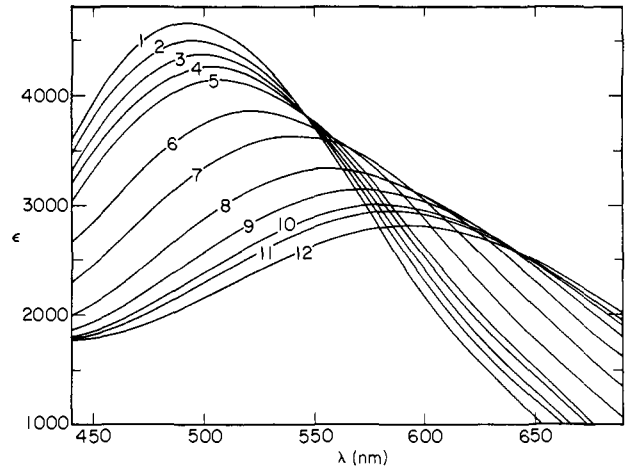

Figure 5. Visible spectra of a 1:1 solution of ferric ion and 3,3,4-CYCAMS as a function of pH: 1, pH 7.46; 2, 7.20; 3, 7.06; 4, 6.93; 5, 6.80; 6, 6.47; 7, 6.13; 8, 5.81; 9, 5.57; 10, 5.40; 11, 5.29; 12, 4.99.

Ferric CYCAMS. The titration curve of a 1:1 solution of ferric ion and CYCAMS, shown in Figure 4, has a sharp break at $a = 3$ (a = moles of base per mole of iron). The appearance of such a break at an odd, integral a value is significant; it shows that the dihydroxybenzoyl side groups of the tricatecholate ligands behave differently from simple bidentate analogues such as DMBS (in which the bidentate ligands coordinate to, and dissociate from, iron(III) as a single group and either release or absorb two hydrogen ions). Thus breaks in the titration curves of simple catecholates appear at *even*, integral a values.[10,17,18] The appearance of a break at $a = 3$ in the ferric CYCAMS system is consistent with previous results on the unsulfonated tricatecholate CYCAM and MECAM, as well as enterobactin itself, which conclusively showed that such complexes are protonated in discrete one-proton steps.[10,13]

The visible spectra of ferric CYCAMS as a function of pH between pH 5.0 and pH 7.5 (Figure 5) are consistent with the stepwise addition of three protons to $[FeCYCAMS]^{6-}$. From $a = 6$ (pH 8) to $a = 5.3$ (pH 6.8), an isosbestic point is observed at 548 nm. From $a = 3$ (pH 5) to $a = 3.8$ (pH 5.5), a second

(17) Avdeef, A.; Sofen, S. R.; Bregante, T. L.; Raymond, K. N. *J. Am. Chem. Soc.* **1978**, *100*, 5362–5370.
(18) Murakami, Y.; Nakamura, K. *Bull. Chem. Soc. Jpn.* **1963**, *36*, 1408–1411.

Table III. Chelate Protonation Constants and Extinction Coefficients for Ferric CYCAMS Complexes

species	$\log K_{MH_nL}$ (spectr)	$\log K_{MH_nL}$ (potent.)	ϵ, M^{-1} cm^{-1} 490 nm	520 nm	560 nm	590 nm
FeCYCAMS			4928	4523	3295	2254
Fe(HCYCAMS)	6.78 (2)	6.92 (6)	3324 (51)	3796 (26)	3892 (25)	3442 (44)
$Fe(H_2CYCAMS)$	5.74 (4)	5.82 (3)	2165 (90)	2707 (132)	3168 (134)	3347 (108)
$Fe(H_3CYCAMS)$	5.54 (7)	5.46 (16)	1934	2141	2502	2611
$Fe(H_4CYCAMS)$	2.3 (1)	2.4 (1)				

isosbestic point is formed at 643 nm. In the intermediate region from $a = 5.3$ to 3.8, no isosbestic point is observed. These results are best explained in terms of the three equilibria eq 8–10. The

$$FeCYCAMS^{6-} + H^+ \overset{K_{MHL}}{\rightleftharpoons} Fe(HCYCAMS)^{5-} \quad (8)$$

$$Fe(HCYCAMS)^{5-} + H^+ \overset{K_{MH_2L}}{\rightleftharpoons} Fe(H_2CYCAMS)^{4-} \quad (9)$$

$$Fe(H_2CYCAMS)^{4-} + H^+ \overset{K_{MH_3L}}{\rightleftharpoons} Fe(H_3CYCAMS)^{3-} \quad (10)$$

initial isosbestic point at 548 nm is a reflection of the protonation of $[FeCYCAMS]^{6-}$ according to eq 8. As the pH is lowered further, reaction 9 becomes a significant factor, and the presence of three metal complexes results in the loss of the isosbestic point. As the pH is lowered further, reactions 8 and 9 eventually go to completion, leaving reaction 10 as the only significant equilibrium. At this point a second isosbestic point appears at 643 nm due to overlap in the absorbance spectra of $[Fe(H_2CYCAMS)]^{4-}$ and $Fe(H_3CYCAMS)]^{3-}$.

Because the protonation equilibria overlap so strongly, the simple type of calculation which was used in the DMBS system is inadequate for the CYCAMS data. Instead, a nonlinear, least-squares refinement was used to calculate extinction coefficients and protonation constants by minimizing the differences between observed and calculated absorbances. At each pH, the absorbances were recorded at 490, 520, 560, and 590 nm. At any wavelength, the absorbance is given by eq 11. The values of [ML]

$$Abs^{\lambda} = [ML] \times (\epsilon_{ML}{}^{\lambda} + K_1(H)\epsilon_{MHL}{}^{\lambda} + K_1K_2(H)^2\epsilon_{MH_2L}{}^{\lambda} + K_1K_2K_3(H)^3\epsilon_{MH_3L}{}^{\lambda}) \quad (11)$$

can be calculated from mass balance by using an initial set of equilibrium constants.

$$[Fe]_{total} = [ML](1 + K_1H + K_1K_2(H)^2 + K_1K_2K_3(H)^3) \quad (12)$$

The values of $\epsilon_{ML}{}^{\lambda_{1-4}}$ and $\epsilon_{MH_3L}{}^{\lambda_{1-4}}$ were obtained directly from the spectra at pH 9 and pH 4.5, since the titration data indicate that these are essentially the only species in solution at these specific pHs. Thus there are a total of 11 variables: $\epsilon_{MHL}{}^{\lambda_{1-4}}$, $\epsilon_{MH_2L}{}^{\lambda_{1-4}}$, K_1, K_2, K_3. These were refined simultaneously by using 84 data points from spectra at 21 pH values between 8.3 and 4.4. The final set of equilibrium constants and extinction coefficients are listed in Table III. The species distribution curves calculated from these constants are shown in Figure 6. Note in particular the relatively rapid formation of the tris(salicylate) species $Fe(H_3CYCAMS)^{3-}$—which indicates an unusual stability for this complex.

The successive protonations of ferric CYCAMS continue below $a = 3$. Equation 13 (vide infra) can also be used to treat the data immediately below $a = 3$ to give a value of $\log K_{MH_4L} = 2.3$. However, overlap with other protonation equilibria limits the pH range of the data, and the uncertainty in this value is thus larger.

Ferric MECAMS. The titration curve of ferric MECAMS in Figure 4 indicates that the chelate protonation constants are much lower than those in the CYCAMS system. The potentiometric data between pH 6.6 and pH 3.0 were refined by nonlinear least squares to give values of $\log K_{MHL} = 5.74$ (2), $\log K_{MH_2L} = 4.10$ (4), and $\log K_{MH_3L} = 3.46$ (5).

As the pH of ferric MECAMS is lowered from 7 ($a \geq 6$) to about 5.1, the visible spectra form a sharp isosbestic point at 542 nm, as shown in Figure 7. Over the range of this isosbestic point, the absorbance at any chosen wavelength can be fit to the equation derived by Schwarzenbach[19] (eq 13), where ϵ_{obsd} is the absorbance

$$\epsilon_{obsd} = \frac{1}{K_{MH_nL}} \frac{(\epsilon_{ML} - \epsilon_{obsd})}{[H]^n} + \epsilon_{MH_nL} \quad (13)$$

at any pH divided by the analytical iron concentration and ϵ_{ML} and ϵ_{MH_nL} are the molar extinction coefficients of the ML and MH_nL species. The n, which appears as the exponent of $1/[H]$, is the stoichiometric coefficient of hydrogen ion for the reaction $ML + nH \rightleftharpoons MH_nL$. The plot of $(\epsilon_{ML} - \epsilon_{obsd})/[H]^n$ vs. ϵ_{obsd} for ferric MECAMS is linear only for $n = 1$, as shown in Figure 8,

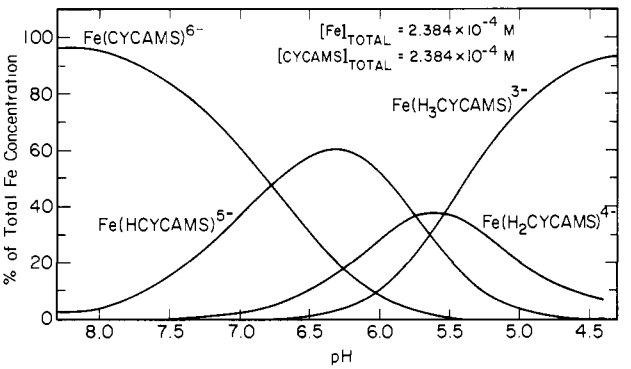

Figure 6. A plot of the species distribution resulting from protonation of $FeCYCAMS^{6-}$. The relative concentration of each species as a percentage of the total iron concentration is shown as a function of pH.

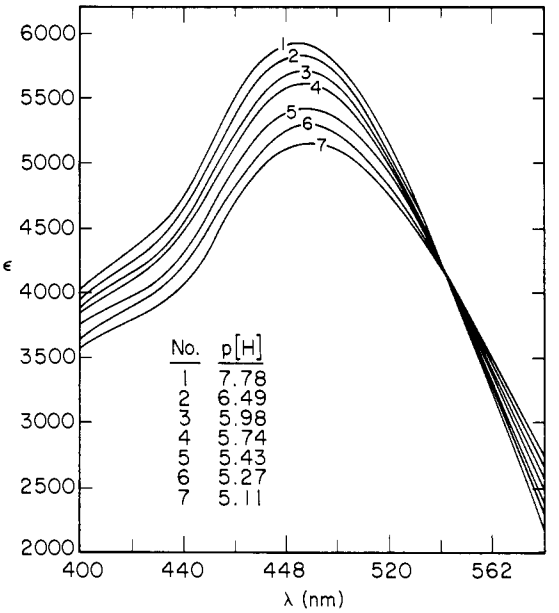

Figure 7. Visible spectra of a 1:1 solution of ferric ion and MECAMS recorded as a function of pH: $[Fe^{3+}]_{total} = 2.8 \times 10^{-4}$; $\mu = 0.10$ M (KNO_3); $T = 25$ °C.

(19) Schwarzenbach, G.; Schwarzenbach, K. *Helv. Chim. Acta* **1963**, *46*, 1390–1400.

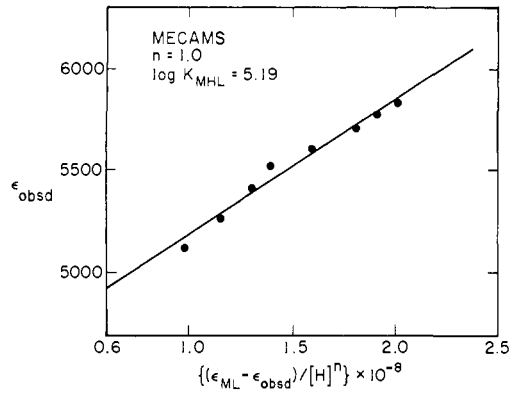

Figure 8. Plot of $(\epsilon_{ML} - \epsilon_{obsd})/[H]^n$ vs. ϵ_{obsd} for ferric MECAMS using $n = 1$, where ϵ_{ML} is the molar extinction coefficient of $[FeMECAMS]^{6-}$ at 485 nm and ϵ_{obsd} is the apparent extinction coefficient at any pH (ϵ_{obsd} = absorbance$_{485}$/total iron). The data cover the pH range 6.47–5.1.

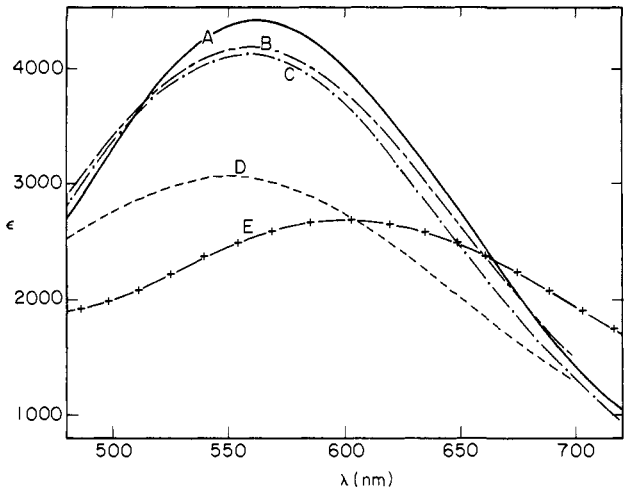

Figure 9. Visible spectra of several metal catecholate complexes: (A) $[Fe(DMBS)_2]^{3-}$ (pH 5.8); (B) $[Fe(H_2TRIMCAMS)]^{4-}$ (pH 6.08); (C) $[Fe(H_2LICAMS)]^{4-}$ (pH 4.8); (D) $[Fe(H_3MECAMS)]^{3-}$ (pH 2.4); (E) $[Fe(H_3\text{-}CYCAMS)]^{3-}$ (pH 4.4).

with a value of log K_{MHL} = 5.19 (3).

Below pH 5, the sequential protonation equilibria overlap such that no further isosbestic points are observed. Instead there is a gradual shift in λ_{max} from 485 nm to ~560 nm at pH 2.5. In the ferric CYCAMS system, the λ_{max} at $a = 3$ (pH 4.4) has shifted further to the red to 600 nm. Both spectra are shown in Figure 9 (curves D and E).

Ferric LICAMS. The potentiometric equilibrium curve for ferric LICAMS is also shown in Figure 4. Unlike the MECAMS and CYCAMS systems, there is a sharp break at $a = 4.0$. The changes in the visible spectra also differ from the other systems discussed above, in that the spectrum recorded at $a = 4$ is very similar to the spectrum of the $(DMBS)_2Fe^{III}$ complex (curves A and C of Figure 9). This similarity suggests that the first two protonations of ferric LICAMS may both involve the same hydroxybenzoyl groups, which dissociates from the metal to leave iron(III) coordinated to the four phenolic oxygens of the two remaining dihydroxybenzoyl groups.

The visible spectra of ferric LICAMS from pH 4.8 ($a = 4$) to pH 7.1 ($a = 6$) form two, sequential isosbestic points, which indicate that these first two protonations occur in sequential one-proton steps. The value of the initial protonation constant K_{MHL} can be calculated from eq 13. We have previously extended this graphical approach by deriving an equation which describes the data over the range of the second, low pH isosbestic point.[13]

$$\epsilon_{obsd} = K_{MH_2L}[H](\epsilon_{MH_2L} - \epsilon_{obsd}) + \epsilon_{MHL} \qquad (14)$$

A value of K_{MH_2L} has been determined from a plot of ϵ_{obsd} vs. $(\epsilon_{MH_2L} - \epsilon_{obsd})[H]$ over the pH range just beyond $a = 4$. Duplicate determinations of both K_{MHL} and K_{MH_2L} have been made by refinement of the potentiometric data between $a = 4$ and $a = 6$. Both sets of constants are listed in Table IV. Also listed are values determined by each method for the third chelate protonation constant. Because log K_{MHL} and log K_{MH_2L} are fairly close together, the pH ranges over which the visible spectra are amenable to graphical analysis are somewhat narrow. Thus the potentiometric values should be considered the more reliable set of constants.

Table IV. Ferric LICAMS Chelate Protonation Constants

	spectrophotometric	potentiometric
log K_{MHL}	5.85 (2)	6.16 (6)
log K_{MH_2L}	5.32 (7)	5.3 (1)
log K_{MH_3L}	3.05 (4)	3.10 (4)

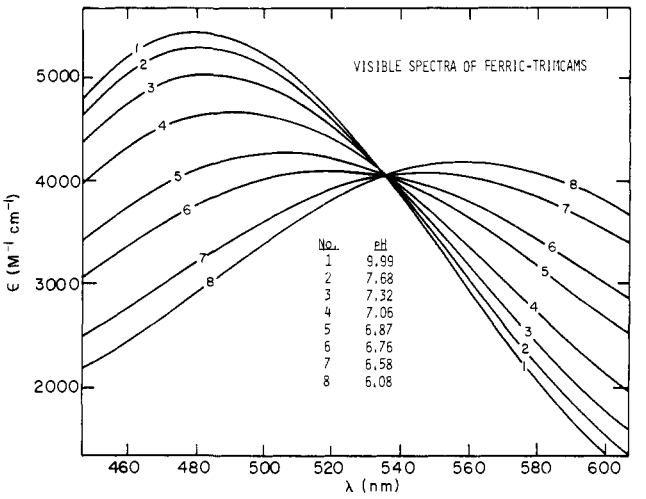

Figure 10. Visible spectra of a 1:1 solution of ferric ion and TRIMCAMS as a function of pH: $[Fe^{3+}]_{total} = 1.5 \times 10^{-4}$ M; $\mu = 0.10$ M (KNO_3); $T = 25$ °C.

Ferric TRIMCAMS. The ferric TRIMCAMS titration curve in Figure 4 resembles the ferric LICAMS system in that there is a sharp break at $a = 4.0$. The fully deprotonated $[FeTRIMCAMS]^{6-}$ complex has a λ_{max} = 480 (ϵ = 5300). As the pH decreases from 8.0, λ_{max} gradually shifts to 560 nm as shown in Figure 10. An important feature of this system is the retention of a single isosbestic point at 536 nm over the entire range from $a = 4$ to $a = 6$. This is strong evidence that the addition of two protons to form $[Fe(H_2TRIMCAMS)]^{4-}$ occurs in a *single*, discrete step and not as two sequential one-proton reactions. Confirmation of this is obtained by graphical analysis of the spectrophotometric data according to eq 13. A linear plot is obtained only for $n = 2$, as shown in Figure 11, yielding a value of

$$K_{MH_2L}{}^2 = \frac{[MH_2L]}{[ML][H]^2} = 10^{13.662(2)} \qquad (15)$$

A value of log $K_{MH_2L}{}^2$ = 13.1 (1) was obtained by least-squares refinement of the potentiometric data.

Spectrophotometric Competitions

The overall formation constants of the iron(III) complexes of the tricatecholate ligands cannot be determined directly because the iron binding is so strong that the complexes are not appreciably dissociated into free ligand and free iron above pH 2. Below this pH, the system is complicated by internal redox reactions that form ferrous semiquinones, which proceed irreversibly to byproducts. Therefore, proton-dependent stability constants have been determined spectrophotometrically by competition with EDTA. Because the three largest ligand protonation constants are unknown, it is not possible to calculate standard formation constants, i.e., those written in terms of the fully deprotonated form of the

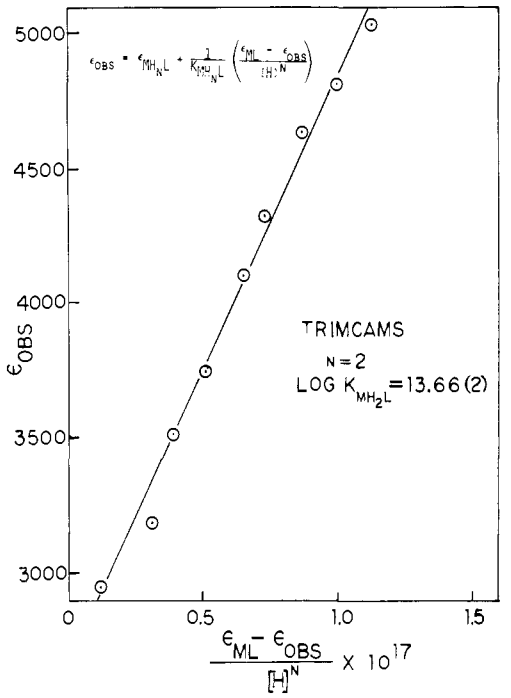

Figure 11. Plot of $(\epsilon_{ML} - \epsilon_{obsd})/[H]^n$ vs. ϵ_{obsd} for ferric TRIMCAMS using $n = 2$, where ϵ_{ML} is the molar extinction coefficient of [FeTRIMCAMS]$^{6-}$ at 480 nm and ϵ_{obsd} is the apparent extinction coefficient at any pH (ϵ_{obsd} = absorbance$_{480}$/total iron). Data cover the pH range 7.32–6.36.

ligand. Instead, the equilibria are expressed in terms of the H_3L species as shown in eq 16 and 17. The K^* values adequately

$$Fe + H_3L = FeL + 3H^+ \quad (16)$$

$$K^* = \frac{[FeL][H]^3}{[Fe][H_3L]} \quad (17)$$

represent the metal–ligand system whenever there are no free ligand species present with less than three phenolic protons. Thus the application of these constants is valid up to pH ~10.5.

A mixture of a tricatecholate (H_6L), Fe^{3+}, and EDTA is described by the eq 18–21. The α's are the usual functions of pH and either ligand or chelate protonation constants.

$$[L]_{total} = \alpha_L[H_3L] + \alpha[FeL] \quad (18)$$

$$[EDTA]_{total} = \alpha_{EDTA}[EDTA^{4-}] + \alpha'[FeEDTA] \quad (19)$$

$$[Fe]_{total} = \alpha[FeL] + \alpha'[FeEDTA] \quad (20)$$

$$Abs^{480} = [FeL](\epsilon_{FeL} + K_{FeHL}[H]\epsilon_{FeHL} + K_{FeHL}K_{FeH_2L}[H]^2\epsilon_{FeH_2L} + K_{FeHL}K_{FeH_2L}K_{FeH_3L}[H]^3\epsilon_{FeH_3L}) \quad (21)$$

Because of the excess ligand present, it was assumed that uncomplexed iron represents a negligible fraction of $[Fe]_{total}$. Also, the charge-transfer bands of the catecholate complexes are so intense relative to the spin-forbidden d–d bands of the ferric EDTA, that one may assume that the absorbance at 480 nm is due solely to the metal catecholate species.

Equations 18–21 may be solved to give [FeL], [FeEDTA], [H_3L], and [EDTA]. These quantities are then used to calculate a distribution coefficient

$$K_x = \frac{[FeL][EDTA][H]^3}{[FeEDTA][H_3L]} = \frac{K^*}{K_{FeEDTA}} \quad (22)$$

One thus obtains values of K^* which are based on the literature value of the normal stability constant of ferric EDTA. Values of log K^* are listed in Table V, along with literature values of analogous unsulfonated ligands. Normal formation constants for these systems may be *estimated* by assuming that the high protonation constants of the tricatecholate ligands have average values of log K = 12.1 for unsulfonated and log K = 11.5 for sulfonated benzamide ligands. These estimated protonation constants are based on literature values reported for simple substituted catechols.[16,17]

Table V. pH Dependent Equilibrium Constants and Normal Formation Constants of a Series of Ferric Complexes

ligand	log K^*	log K_{ML} (est)
enterobactin[a]	15.7	52
MECAMS	6.57 (10)	41
LICAMS	6.40 (9)	41
TRIMCAMS	4.43 (14)	41
CYCAMS	3.44 (10)	38
MECAM[b]	9.5 (3)	46
CYCAM[b]	3.4 (1)	40

[a] Reference 10. [b] Reference 13.

Discussion

Ligand Protonation Constants. The second protonation constant of DMBS is $10^{7.26}$, compared to $10^{8.4}$ for the unsulfonated analogue, (2,3-dihydroxybenzoyl)-*N*,*N*-dimethylbenzamide. This is consistent with the change in protonation constant between catechol (log K = 9.2) and 4-sulfocatechol (log K = 8.3). Thus the inductive effect of the sulfonate group lowers the protonation constant of an aromatic hydroxyl group by about 1 log unit.

The ligand protonation constants of the tricatecholates are reasonably consistent with the DMBS value, with average log K values of 7.3 ± 0.7. The TRIMCAMS protonation constants are larger than those of the other ligands since there is no carbonyl group α to the dihydroxybenzene rings. On the basis of the difference in acidity between catechol (log K = 9.2) and 2,3-dihydroxy-*N*,*N*-dimethylbenzamide (log K = 8.4), the carbonyl group appears to lower catecholate protonation constants by ~0.8 log unit. If the TRIMCAMS values are corrected by this amount, the average log K is 7.3, essentially identical with the DMBS constant. Thus there do not appear to be any significant intramolecular interactions between the three dihydroxybenzoyl groups in the tricatecholate ligands. This generalization logically extends to enterobactin as well, for which no protonation constants are known, and indicates that the enhanced effectiveness of this ligand at physiological pH is probably not related to any substantial reduction in ligand pK_a's.

Ferric Complex Protonations. The vis–UV absorption spectra of simple mono-, bis- and tris(catecholato)iron(III) complexes have widely separated maxima, with ranges of 480–495 nm for the tris and 560–570 nm for the bis complexes. The spectra of the ferric complexes of these tricatecholate ligands at high pH closely resemble that of $(DMBS)_3Fe^{III}$, with $480 < \lambda_{max} < 490$ nm and $5000 < \epsilon < 6000$ M^{-1} cm^{-1}. These spectroscopic data, plus the titration of a total of 6 equiv of hydrogen ion below pH 10 in the presence of equimolar ferric ion, are an indication of coordination via the six phenolic oxygens of the three dihydroxybenzoyl side groups.

Although all the tricatecholate ligands form the same type of complex at high pH, the protonation equilibria observed as the pH is increased are strongly dependent on the ligand structure. Bidentate catecholate ligands almost invariably coordinate and dissociate as a unit and in the process either release or consume 2 equiv of hydrogen ion.[10,17,18,20] However, the linearity of plots of eq 13 and 14 with n values of 1.0 indicates that the ferric complexes of LICAMS and MECAMS are protonated in *one-proton* steps. There are several other observations which are consistent with such a model: the number of isosbestic points observed, the pH range over which they exist, the break in the titration curve of ferric CYCAMS at a = 3, and the satisfactory refinement of all the potentiometric data using this model.

The protonation of the ferric complex of the unsulfonated MECAM also proceeds in one-proton steps. It has been shown by solid-state IR studies that the protonation of the red, hexa-

(20) Dubey, S. N.; Mehrotra, R. C. *J. Inorg. Nucl. Chem.* **1964**, *26*, 1543–1550.

coordinate $[FeMECAM]^{3-}$ complex produces a shift in the mode of bonding from one in which the iron is coordinated to the two phenolic oxygens of each dihydroxybenzoyl group (catecholate mode) to one in which the iron is bound to the ortho phenolic and amide carbonyl oxygens (salicylate mode), as shown in eq 23.[13]

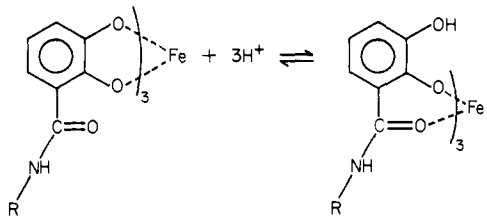

(23)

The TRIMCAMS results reported here provide additional support for such a shift in the mode of bonding. This ligand is an isomer of MECAMS in which the carbonyl groups are no longer α to the dihydroxybenzene rings; instead, all three carbonyls in TRIMCAMS are adjacent to the central benzene ring (see the structures in Figure 1). Thus the carbonyl oxygen is no longer able to form a stable six-membered chelate ring with the ortho phenol and is sterically prevented from binding to iron. As a result of this one structural variation, the ferric complex of TRIMCAMS reacts with hydrogen ion in *two-proton* steps. In addition, the absorbance maximum of ferric TRIMCAMS as a function of pH shifts from 490 to 560 nm, with a single, sharp isosbestic point preserved over this entire region. Such behavior is clearly analogous to simple catechol complexes and is easily explained as resulting from the double protonation and concomitant dissociation of one of the (dihydroxybenzyl)amide side groups. Thus one-proton reactions are observed *only* when there is an α-carbonyl group ortho to one of the catecholate oxygens.

The rather straightforward changes in the visible spectrum of the ferric DMBS system are so similar to those of catechol itself that one can safely rule out any involvement of the amide carbonyl oxygen in iron binding, in apparent contradiction to the results just described for the tricatecholates. However, a key difference between the tricatecholates and DMBS is the number of molecules involved in the complexation equilibria. The disproportionation of a salicylate complex of a tricatecholate ligand would be expressed as

$$2[Fe(HL)] \overset{K_{dis}}{\rightleftharpoons} FeL + FeH_2L \qquad (24)$$

The results discussed above indicate that this equilibrium lies well to the left. The analogous reaction for the DMBS system is expressed as

$$2[Fe(DMBS)_2(HDMBS)] \overset{K_{dis}'}{\rightleftharpoons} Fe(DMBS)_2 + Fe(DMBS)_3 + H_2DMBS \qquad (25)$$

The concentration dependence of eq 25 tends to favor disproportionation of any DMBS "salicylate" complex under the very dilute conditions employed in this study. These effects have been discussed in detail elsewhere.[10]

Formation Constants. The proton-dependent constants (K^*) listed in Table V do not appear to be very large because they are written in terms of the H_3L form of the ligand. Using reasonable estimates for the average value of the last three ligand protonation constants, we can estimate the value of the standard formation constant ($K_{ML} = [FeL]/[Fe][L]$), and these values are also listed in Table V. The K_{ML} values clearly reflect the exceptional stability of these complexes. As a comparison, ferric EDTA has a log K_{ML} of only 25, some 15–20 *orders of magnitude* smaller than the catecholate compounds.

The relatively low stability constants for both CYCAMS and CYCAM are indicative of considerable strain associated with the complete encapsulation of ferric ion. This presumably results from having the amide nitrogens contained within the 13-membered central ring. In both enterobactin and MECAMS, the nitrogens are exocyclic, which results in longer bridging groups between the exterior 2,3-dihydroxybenzoyl rings and the central triester ring of enterobactin or benzene ring of MECAMS.

Table VI. Equilibrium Free Metal Ion Concentrations Expressed as pM = –log $[Fe^{3+}]$

ligand	pM[a]	ligand	pM[a]
enterobactin	35.5	TRIMCAMS	25.1
HBED[b]	31.0	CYCAMS	24.9
MECAMS	29.4	DTPA[d]	24.7
MECAM	29.1	transferrin	23.6
LICAMS	28.5	CYCAM	23.0
ferrioxamine B	26.6	EDTA[e]	22.2
EHPG[c]	26.4	tiron[f]	19.5
ferrichrome A	25.2	DMBS	19.2

[a] Calculated for 10 μM ligand, 1 μM Fe^{3+}, pH 7.4. [b] *N,N'*-bis-(2-hydroxybenzyl)ethylenediamine-*N,N'*-diacetic acid.[21] [c] Ethylene-1,2-bis(2-hydroxyphenylglycine).[22] [d] Diethylenetriaminepentaacetic acid. [e] Ethylenediaminediacetic acid. [f] 1,2-Dihydroxy-3,5-disulfobenzene.

There is a surprisingly large increase in the proton-dependent formation constant (log K^*) value of MECAMS compared to TRIMCAMS, especially considering that the higher ligand protonation constants of TRIMCAMS would tend to increase its log K^*. As discussed above, there is only an isomeric structural variation between TRIMCAMS and MECAMS, as shown. Thus

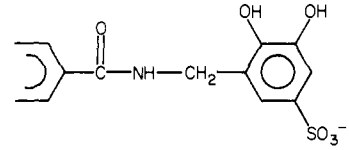

TRIMCAMS

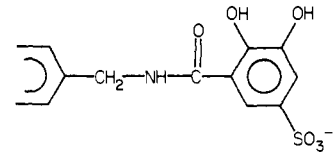

MECAMS

the overall formation constants appear to be very sensitive to changes in the structure of the ligand. We suspect that the exceptionally high stability constant for enterobactin is due in large part to the conformational flexibility of the triester ring, as compared to the rigidly planar benzene platform in MECAMS and TRIMCAMS. It may even be that the triester group is predisposed toward a conformation favorable to the optimal arrangement of the coordinating groups about the ferric ion.

Although the formation constants of the catecholate complexes are exceptionally large, the coordinating phenolic oxygens are such weak acids that the full effect of log K_{ML} would be observed only when $[OH^-]$ is at least 1 M. At physiological pH, hydrogen ion will compete with iron for bonding to the phenolate oxygens, so that the effectiveness of the catecholate ligands drops rapidly with increasing acidity. Clearly log K_{ML} is a poor standard by which to measure the effectiveness of a potential iron removal agent at physiological pH. Therefore, we have calculated the concentrations of unchelated, hexaaquoiron(III) in a solution which is 10 μM in ligand, 1 μM in metal, at pH 7.4. These are expressed as pM, where pM = –log $[Fe(H_3O)_6^{3+}]$, and are listed in Table VI for the catecholate ligands, along with some other important synthetic and biological ligands. The comparison between different ligands is now straightforward: the larger the pM value, the more effective the ligand under these prescribed conditions. The use of pM values for comparing the relative effectiveness of ligands has the added advantage of readily accommodating systems which have additional equilibria such as hydrolyses or dimerizations, which affect the iron concentration but are not reflected in log K_{ML} values. Also, in the catecholate systems one can calculate pM values without using the inherently inaccurate estimates of the three most basic ligand protonation constants, which are required to obtain a value of K_{ML}.

The pM value of 35.5 shows enterobactin to be the most effective ligand for iron(III) ever characterized. It is some 10 000

times more effective than any of the synthetic ligands and is $\sim 10^8$ times more effective than any of the hydroxamate siderophores.

The pM values of the sulfonated catecholates range from 24.9 from CYCAMS to 29.4 for MECAMS. The catecholates are clearly superior to the aminocarboxylate ligands such as DTPA (pM 24.7) and EDTA (pM 22.2). The pM values of the two most effective catecholates, LICAMS and MECAMS, are even higher than those of the hydroxamate siderophores. Other than enterobactin itself, the only ligands with sequestering ability equal to the sulfonated catecholates are the diphenolic ligands prepared and evaluated by Martell.[21,22] Of these, EHPG has shown some promise on the basis of in vivo iron removal studies,[23] even though its pM is a relatively modest 26.4.

A comparison of the pM values of the bidentate ligands tiron and DMBS with those of the tricatecholates clearly shows the importance of the possible number of coordination sites occupied by a ligand in determining its effectiveness at very dilute concentrations. The log β_3* for DMBS is 5.8, which is less than 1 log unit below the log K*'s of MECAMS and LICAMS and is actually higher than the log K*'s of TRIMCANS and CYCAMS. Its pM value, however, is a full 10 log units below MECAMS and LICAMS. This is an important consideration, since in vivo iron removal must of necessity entail low ligand concentrations.

Iron is stored in the body by two proteins, ferritin and hemosiderin. Both consist of a hydroxide–oxide–phosphate–iron(III) core surrounded by protein subunits,[24] and it is unlikely that simple chelating agents will remove significant amounts of this iron. However, transferrin, which is the plasma iron-transport protein, binds to specific receptor sights on ferritin and can readily mobilize this storage iron.[25] Thus the most likely mechanism for successful iron removal is to administer chelating agents which will remove the iron from transferrin and facilitate its excretion from the body and then allow the apotransferrin to mobilize the less accessible iron stores. Obviously the key factor in such an approach is finding a drug which will remove iron from transferrin. Transferrin has a pM value of only 23.6. From inspection of Table VI it is clear that almost all the catecholate ligands are capable thermodynamically of removing iron from transferrin. In the case of MECAMS, the competition equilibrium with transferrin favors the catecholate ligand by about 10^6, and even CYCAMS, which is the least effective of the sulfonated catecholates, is favored thermodynamically by a factor of 20. Thus it is obvious that the sulfonated catecholates represent a class of ligands which easily satisfy the thermodynamic requirements for a potential iron removal agent.

Since desferrioxamine B has a pM of 26.6, it also is thermodynamically capable of removing iron from transferrin. However, this exchange reaction is in fact too slow to be of clinical importance.[11] We have investigated the kinetics of iron removal from transferrin by several tricatecholate ligands and have found the reaction to proceed much more rapidly, with ~50% iron removal in 30 min. The details of this study have been reported separately.[11]

Summary

The sulfonated tricatecholates have been shown to combine a number of features which are necessary for an effective iron-sequestering agent. They are water soluble and are more resistant to air oxidation than their unsulfonated analogues. Unlike enterobactin, they are hydrolytically stable over a wide pH range. The lower ligand protonation constants of the sulfonated catecholates enhance their effectiveness at physiological pH. In particular, LICAMS and MECAMS are among the most effective iron ligands ever characterized. Finally, the catechols in general are capable of removing iron from transferrin at a reasonable rate under conditions where ferrioxamine B is almost totally ineffective. Animal tests of the in vivo efficacy of these compounds for iron decorporation are in progress, and the results will be reported separately.

Acknowledgment. We wish to thank Mary Kappel for her assistance in the least-squares analysis of the spectrophotometric data. This research is supported by the NIH through Grant HL 24775.

(21) L'Epllatenier, F.; Murase, I.; Martell, A. E. *J. Am. Chem. Soc.* **1967**, *89*, 837–843.
(22) Frost, A. E.; Freedman, H. H.; Westerback, S. J., Martell, A. E. *J. Am. Chem. Soc.* **1958**, *80*, 530–536.
(23) Pitts, C. G.; Gupta, G.; Estes, W. E.; Rosenkrantz, H.; Metterville, J. J.; Crumbliss, A. L.; Palmer, R. A.; Nordquest, K. W.; Hardy, K. A. S.; Whitcombe, D. R.; Byers, B. R.; Arceneaux, J. E. L.; Gaines, C. G.; Sciortino, C. V. *J. Pharmacol. Exp. Ther.* **1979**, *208*, 12–18.
(24) Ochiai, E. "Bioinorganic Chemistry"; Allyn and Bacon: Boston, 1977; p 171.
(25) Beck, W. S. "Hematology"; Massachusetts Institute of Technology, 1974; p 38.

Electron-Rich Carboranes. Studies of a Stereochemically Novel System, $(CH_3)_4C_4B_7H_9$, an 11-Vertex Arachno Cluster[1]

David C. Finster and Russell N. Grimes*

Contribution from the Department of Chemistry, University of Virginia, Charlottesville, Virginia 22901. *Received September 8, 1980*

Abstract: The controlled degradation of $(CH_3)_4C_4B_8H_8$ (I) in 95% ethanol in air gives $(CH_3)_4C_4B_7H_9$ (II). Electrophilic bromination of II produces 11-Br$(CH_3)_4C_4B_7H_8$ (III), which is shown in an X-ray diffraction study to have an open-cage structure with a bridging -CH(CH_3)- group across the open face; compounds II and III can be described as 11-vertex arachno cages. Deprotonation of II with NaH in THF generates the monoanion $(CH_3)_4C_4B_7H_8^-$ (IV) from which the CH proton on the bridging group has been removed. Protonation of IV gives a new isomer of $(CH_3)_4C_4B_7H_9$ (V), whose ^{11}B and ^{1}H FT NMR spectra indicate a substantially different cage geometry from that of II. The molecular structures of II–V and pathways for their interconversion are discussed in light of NMR, IR, mass spectroscopic, and X-ray evidence. Crystal data for III: $BrC_8B_7H_{20}$; mol wt 271.84; space group $P\bar{1}$; $Z = 2$; $a = 7.764$ (3), $b = 8.352$ (5), $c = 12.317$ (6) Å; $\alpha = 94.53$ (5), $\beta = 95.41$ (5), $\gamma = 120.51$ (5)°; $V = 678$ Å^3; $R = 0.057$ for 1404 independent reflections having $F_o^2 > 3\sigma(F_o^2)$.

The high-yield preparation[2] of the tetracarbon carborane $(CH_3)_4C_4B_8H_8$ (I) has opened up new, intriguing avenues in boron cage synthesis, and a variety of 11- to 14-vertex metallacarboranes has been obtained[3] by insertion of transition metals into I, both

0002-7863/81/1503-2675$01.25/0